

## PROPAGATION IN LINEAR ARRAYS OF PARALLEL WIRES\*

J. R. Pierce

Bell Telephone Laboratories, Inc., Murray Hill, N.J.

Consider an array of parallel perfectly-conducting wires extending between and normal to two infinite parallel perfectly-conducting planes. One wire acts as a resonator, having natural frequencies at which it is an integral number of half-wavelengths long. One might at first think that  $n$  wires would have  $n$  times as many natural frequencies. It turns out, however, that the modes characteristic of the system of many wires are plane electromagnetic waves with the field normal to the wires. All the modes of the array have frequencies for which the wires are an integral number of half-wavelengths long. In circuit terms, the wires, which act as resonators, are uncoupled. The electric and magnetic couplings are equal and opposite.

L. R. Walker has used a linear array of equally-spaced wires as a circuit for an "easitron", a distributed form of unloaded multi-resonator klystron; this work has not been published.

A. Karp has found that if the array of wires extends across a slot cut in a conducting plane, as in Fig. 1a, or across a channel milled in a conducting block, as shown in Fig. 1b, the wires are coupled somewhat, and the structure forms a circuit which will sustain progressive waves. This coupling must come about because the fields, and particularly the magnetic field near the ends of the wires, are a little different from the fields for wires between infinite parallel planes, and so the electric and magnetic couplings do not quite cancel.

It is found that by adding a central ridge as shown in Fig. 1c the net coupling between wires is increased, presumably through changes in the electric field.

Karp has found structures of the form shown in Fig. 1 useful in millimeter-wave backward-wave oscillators when used with spatial-harmonic interaction such that the effective phase shift between wires is  $-2\pi + \theta$  radians, where  $\theta$  is the fundamental phase shift between wires.<sup>1</sup> As yet, it has not been possible to calculate the behavior of these structures. However, an approximate treatment of the effect of the central ridge alone will be given in this paper. A related case, in which the ridge is replaced by a groove, and in which the fundamental component of the field is a backward wave, is also treated.

### 1. Phase Constant for Structures Similar to Karp's

Fig. 2 shows the structure similar to Karp's which is used in the analysis. An array of wires lying in the  $x$ -direction extends between

\*An analysis of a similar structure was presented by A. Leblond and G. Mourier, "Étude des Lignes à Barreaux à Structure Périodique (2<sup>e</sup> partie)," *Annales de Radioélectricité*, Vol. IX, pp. 311-328, October, 1954.

infinite parallel planes  $P_1$  and  $P_2$ . In the analysis this array is replaced by a sheet which conducts in the  $x$  direction but not in the  $z$  direction, which is normal to the plane of the paper.

Below the wires ( $y < 0$ ), at a distance  $y_0$  from the wires, there is a conducting bar of width  $2a$ . The plane  $P_1$  is a distance  $b$  to the left of the side of the bar, so that the spacing between planes  $P_1$  and  $P_2$  is  $2(a+b)$ .

The plan is to assume transverse electromagnetic waves in the  $x$  direction with no electric or magnetic field in the direction of the wires, both in the regions to the left and to the right of the bar, and also in the region above the bar, and to match boundary conditions approximately at the edges of the bar. This matching consists of assuming that  $E_z$  must be the same at both sides of the edge of the central bar, and that the current in the wires (or sheet) must be the same on both sides of this edge. This current is given by the difference between  $H_z$  above the wires ( $y > 0$ ) and  $H_z$  below the wires ( $y < 0$ ).

We will let subscript 1 denote field components below the wires and subscript 2 denote field components above the wires. In the center region, above the bar,  $y > -y_0$  ( $-a < x < a$ ) we measure  $x$  from the center line. The fields  $E_z$  and  $E_y$  can be expressed as the derivatives with respect to  $z$  and  $y$  of a function  $\pi$ .<sup>2</sup> This function and all field components are assumed to contain a factor

$$e^{-j\beta z}$$

The functions  $\pi_1$  and  $\pi_2$ , for the center region above and below the wires are

$$\pi_1 = A \frac{\sinh \beta(y+y_0)}{\sinh \beta y_0} \cos kx \quad (1.1)$$

$$\pi_1 = A e^{-\beta y} \cos kx \quad (1.2)$$

$$k = \omega \sqrt{\mu \epsilon} \quad (1.3)$$

The functions  $\pi$  have been adjusted to make  $E_{z1} = E_{z2}$  at  $y = 0$ . The electric field components are

$$E_{z1} = -j\beta A \frac{\sinh \beta(y+y_0)}{\sinh \beta y_0} \cos kx \quad (1.4)$$

$$E_{z2} = -j\beta A e^{-\beta y} \cos kx \quad (1.5)$$

$$E_{y1} = \beta A \frac{\cosh \beta(y+y_0)}{\sinh \beta y_0} \cos kx \quad (1.6)$$

$$E_{y2} = -\beta A e^{-\beta y} \cos kx \quad (1.7)$$

The magnetic field components can be obtained:

$$H_{z1} = \frac{j}{\omega \mu} \frac{\partial E_{y1}}{\partial x} = \frac{-j\beta k}{\omega \mu} A \frac{\cosh \beta(y+y_0)}{\sinh \beta y_0} \sin kx \quad (1.8)$$

Using (1.3), we see that

$$H_{z1} = -j \sqrt{\frac{\epsilon}{\mu}} \beta A \frac{\cosh \beta(y+y_0)}{\sinh \beta y_0} \sin kx \quad (1.9)$$

Similarly

$$H_{z2} = j \sqrt{\frac{\epsilon}{\mu}} \beta A e^{-\beta y} \sin kx \quad (1.10)$$

At  $y = 0$

$$\Delta H_z = H_{z2} - H_{z1} = j \sqrt{\frac{\epsilon}{\mu}} \beta A \left( \frac{\cosh \beta y_0}{\sinh \beta y_0} + 1 \right) \sin kx \quad (1.11)$$

In the region to the left of the edge, i.e.,  $-(a+b) < x < -a$  and  $y > -y_0$  we measure  $x_1$  (which replaces  $x$ ) from the plane  $P_1$ . We obtain

$$\pi_1 = B e^{\beta y} \sin kx_1 \quad (1.12)$$

$$\pi_2 = B e^{-\beta y} \sin kx_1 \quad (1.13)$$

$$E_{z1} = -j\beta B e^{\beta y} \sin kx_1 \quad (1.14)$$

$$E_{z2} = -j\beta B e^{-\beta y} \sin kx_1 \quad (1.15)$$

$$H_{z1} = j \sqrt{\frac{\epsilon}{\mu}} \beta B e^{\beta y} \cos kx_1 \quad (1.16)$$

$$H_{z2} = j \sqrt{\frac{\epsilon}{\mu}} \beta B e^{-\beta y} \cos kx_1 \quad (1.17)$$

At  $y = 0$

$$\Delta H_z = H_{z2} - H_{z1} = -2j \sqrt{\frac{\epsilon}{\mu}} \beta B \cos kx_1 \quad (1.18)$$

At the left end of the bar or ridge

$$x = -a, x_1 = b \quad (1.19)$$

At this point and at  $y = 0$ , we make  $E_z$  and  $\Delta H_z$  the same for the two regions. This gives us from (1.4), (1.14), (1.17) and (1.18)

$$-j\beta A \cos ka = -j\beta B \sin kb \quad (1.20)$$

$$-j \sqrt{\frac{\epsilon}{\mu}} \beta A (\coth \beta y_0 + 1) \sin ka = -2j \sqrt{\frac{\epsilon}{\mu}} \beta B \cos kb \quad (1.21)$$

These yield

$$1 + \coth \beta y_0 = 2 \cot ka \cot kb$$

$$\beta y_0 = \coth^{-1}(2 \cot ka \cot kb - 1) \quad (1.22)$$

Let  $p$  be the distance between wires. The phase angle  $\theta$  between wires is

$$\theta = \beta p \quad (1.23)$$

Let  $\omega_0$  be the radian frequency at which the wires are a half wavelength long. Let

$$\frac{2\pi}{\lambda_0} a = \frac{\omega_0}{c} a = \Phi \quad (1.24)$$

Then, using (1.22), (1.23) and (1.24) we see that

$$\theta = \frac{p}{y_0} \coth^{-1} \left[ 2 \cot\left(\frac{\omega}{\omega_0} \Phi\right) \cot\left(\frac{\omega}{\omega_0} \left(\frac{\pi}{2} - \Phi\right)\right) - 1 \right] \quad (1.25)$$

We see that  $\theta$  as a function of  $\Phi$  is symmetrical about  $\Phi = \pi/4$ . Hence, any extreme value of  $\theta$  must occur at  $\Phi = \pi/4$ . When

$$\Phi = \pi/4 \quad (1.26)$$

$$\theta = \frac{p}{y_0} \coth^{-1} \left[ 2 \cot^2\left(\frac{\omega}{\omega_0} \frac{\pi}{4}\right) - 1 \right] \quad (1.27)$$

In Fig. 3,  $\theta(y_0/p)$  is plotted vs  $\omega/\omega_0$  for  $\Phi = \pi/4$  (upper curve) and for  $\Phi = \pi/3$  or  $\pi/6$  (lower curve).

The higher the curve of  $\theta$  vs  $\omega/\omega_0$ , the "broader the band." Thus,  $\Phi = \pi/4$ , or a ridge half the wire length, is an optimum, but a ridge  $1/3$  or  $2/3$  the wire length isn't very much worse. We see also, the greater is  $p/y_0$ , that is, the smaller is  $y_0$ , the greater will  $\theta$  be, and hence the "broader the band."

Equations (1.25) and (1.27) are of course inaccurate as  $\theta$  approaches  $\pi$ , at which phase angle the array of wires, unlike the uniform sheet assumed, cuts off.

## 2. Fundamental Backward-Wave Structure

Fig. 4a shows a structure in which a central ridge R approaches the wires in region B, while region A is rectangular.

One might make a symmetrical version of the structure as shown in Fig. 4b, with ridges  $R_1$  and  $R_2$  above and below, and region A like region B. This version has, however, a fast TE mode, for the structure with the wires removed is not cut off at the operating frequency, which is a little below that at which the wires are a half free-space wavelength long.

In the symmetrical structure of Fig. 4c, the structure is cut off when we remove the wires. With the wires present there is a slow wave at frequencies a little above that for which the wires are a half a free-space wavelength long.

This structure is a backward-wave circuit; it has a negative phase constant just above the cutoff frequency which assumes a smaller negative value as frequency rises.

Fig. 5 shows the simplified model of the structure which is used in making calculations. Because of the symmetry, we need consider fields on one side of the wires only. Below the wires, in the central region

$$\pi = Ae^{\beta y} \cos kx \quad (2.1)$$

$$E_z = -j\beta Ae^{\beta y} \cos kx \quad (2.2)$$



$$H_z = -j \sqrt{\frac{\epsilon}{\mu}} \beta A e^{\beta y} \sin kx \quad (2.3)$$

In the left-hand region, below the wires

$$\pi = B \frac{\sinh \beta(y+y_0)}{\sinh \beta y_0} \sin kx_1 \quad (2.4)$$

$$E_z = -j\beta B \frac{\sinh \beta(y+y_0)}{\sinh \beta y_0} \sin kx_1 \quad (2.5)$$

$$H_z = j \sqrt{\frac{\epsilon}{\mu}} \beta B \frac{\cosh \beta(y+y_0)}{\sinh \beta y_0} \cos kx_1 \quad (2.6)$$

At  $y = 0$ ,  $x = -a$ ,  $x_1 = b$  we make  $E_z$  and  $H_z$  the same for the two regions. This gives us two equations

$$-j\beta A \cos ka = -j\beta B \sin kb \quad (2.7)$$

$$j \sqrt{\frac{\epsilon}{\mu}} \beta A \sin ka = j \sqrt{\frac{\epsilon}{\mu}} \beta B \coth \beta y_0 \cos kb \quad (2.8)$$

From (2.7) and (2.8) we obtain

$$\coth \beta y_0 = \tan ka \tan kb$$

$$\beta y_0 = \coth^{-1} (\tan ka \tan kb) \quad (2.9)$$

or

$$\beta y_0 = \tanh^{-1} (\cot ka \cot kb) \quad (2.10)$$

As before, we can write

$$\theta = \frac{p}{y_0} \tanh^{-1} \left[ \cot\left(\frac{\omega}{\omega_0} \Phi\right) \cot\left(\frac{\omega}{\omega_0} \left(\frac{\pi}{2} - \Phi\right)\right) \right] \quad (2.11)$$

This makes it appear that  $\theta$  should be positive. We would however have obtained (2.11) if we had assumed a variation with distance as

$$e^{j\beta z}$$

The equations appear not to know which way the wave is going. We know however that for energy flow in the +z direction,  $\theta$  must increase with frequency.

As before,  $\theta$  will have a maximum with respect to  $\Phi$  for  $\Phi = \pi/4$ , and when this is so

$$\theta = \frac{p}{y_0} \tanh^{-1} \left\{ \cot^2 \left( \frac{\omega}{\omega_0} \frac{\pi}{4} \right) \right\} \quad (2.12)$$

In Fig. 6,  $\theta$  from (2.11) is plotted vs  $\omega/\omega_0$ .

Equation (2.11) allows  $\theta$  to pass through 0 and change sign as  $\omega$  is increased. An analysis made assuming a finite height in the central region as in Fig. 4C shows that the structure is actually a band-pass circuit, passing only frequencies lying between  $\omega = 0$  and the value of  $\omega$  for which  $\theta$  is zero.

### 3. Power Flow and Impedance

The usual way of calculating power flow is by means of the Poynting vector. In the approximation we have used, there is no electric or magnetic field in the x direction; hence, the Poynting vector in the z direction must be zero. How can there be power flow?

Actually, there will be transverse components of electric field (and presumably of magnetic field as well) near the edges of the ridge or bar, as indicated by the arrows in Fig. 7. These fields near the edge of the ridge account for the power flow, and associated with them there is a longitudinal current near the edges of the ridge.

The Poynting vector is the cross product of the electric and magnetic fields. Toward the center, the magnetic field is weak; toward the edge the electric field is weak. We might expect the edge of the ridge to be most effective about half way between the center line and the wall, where neither the electric field nor the magnetic field is weak. This is just what we have found.

To calculate power flow by means of the Poynting vector would require a better approximation to the fields than we have used. Another course is open to us, however. We can calculate the group velocity and the stored energy and obtain the power flow as their product.

#### 3.1 Group Velocities

The group velocity  $v_g$  is given by

$$v_g = \frac{1}{\frac{\partial \beta}{\partial \omega}} \quad (3.1)$$

Here we will calculate the group velocity only for the optimum case of  $\Phi = \pi/4$ , using (1.27) for the structure like Karp's and (2.11) for the fundamental backward-wave structure, noting that the sign in (2.11) is wrong. By differentiation and trigonometric transformation we obtain for the structure like Karp's

$$v_g = 8 f_o y_o \frac{\cos(\frac{\omega}{\omega_o} \frac{\pi}{2})}{\tan(\frac{\omega}{\omega_o} \frac{\pi}{4})} \quad (3.2)$$

Here  $f_o$  is the frequency at which the wires are half a free-space wavelength long

$$f_o = \frac{\omega_o}{2\pi} \quad (3.3)$$

For the other structure we obtain

$$v_g = -4 f_o y_o \frac{\cos(\frac{\omega}{\omega_o} \frac{\pi}{2})}{\text{ctn}(\frac{\omega}{\omega_o} \frac{\pi}{4})} \quad (3.4)$$

### 3.2 Stored Energy

The energy stored will be calculated approximately. The electric stored energy  $W_E$  per unit length in the  $z$  direction is calculated for an array of wires, between planes  $P_1$  and  $P_2$ , with no ridge, assuming a sinusoidal variation of electric field with  $x$ . It should be noted that the wire length is

$$\frac{c}{2 f_o} = \frac{1}{2 f_o \sqrt{\mu\epsilon}} \quad (3.5)$$

The actual stored energy will be somewhat higher because of the ridge.

We find that

$$W_E = \frac{E_z^2 \sqrt{\epsilon/\mu}}{8 f_o \beta} \quad (3.6)$$

Here  $E_z$  is, as before, the peak field in the  $z$  direction at the center of the wires. The total stored energy, electric plus magnetic, will be twice  $W_E$ .

### 3.3 Impedances

The longitudinal impedance  $K$  is given by



$$K = \frac{E_z^2}{2\beta^2 P} = \frac{E_z^2}{4\beta^2 v_g W_E} \quad (3.7)$$

We can use  $\beta$  as given by (1.27) and (2.11),  $v_g$  as given by (3.2) and (3.4) and  $W_E$  as given by (3.6) to obtain the impedances for the structure like Karp's and for the fundamental backward-wave structure. For the structure like Karp's we obtain

$$K = \frac{1}{4} \sqrt{\frac{\mu}{\epsilon}} \left\{ \cos\left(\frac{\omega}{\omega_0} \frac{\pi}{2}\right) \operatorname{ctn}\left(\frac{\omega}{\omega_0} \frac{\pi}{4}\right) \coth^{-1} \left[ 2 \operatorname{ctn}^2\left(\frac{\omega}{\omega_0} \frac{\pi}{4}\right) - 1 \right] \right\}^{-1} \quad (3.8)$$

For the other structure we obtain, noting that the signs for  $\beta$  and  $v_g$  are wrong

$$K = - \frac{1}{2} \sqrt{\frac{\mu}{\epsilon}} \left\{ \cos\left(\frac{\omega}{\omega_0} \frac{\pi}{2}\right) \tan\left(\frac{\omega}{\omega_0} \frac{\pi}{4}\right) \tanh^{-1} \left\{ \operatorname{ctn}^2\left(\frac{\omega}{\omega_0} \frac{\pi}{4}\right) \right\} \right\}^{-1} \quad (3.9)$$

We should note that

$$\sqrt{\frac{\mu}{\epsilon}} = 377 \text{ ohms} \quad (3.10)$$

The impedances as given by (3.8) and (3.9) will be too high for small values of  $\theta$  because the added capacitance due to the ridge has been neglected.

In Figs. 8 and 9 the impedances of (3.8) and (3.9) are plotted vs  $\omega/\omega_0$ .

It is unfortunate that the impedance of Fig. 8 for the forward-wave circuit is the impedance for the forward wave, and not for the backward wave in which we are interested. To get the impedance for the backward wave one would have to consider the spatial harmonics caused by the wires or tapes which we have here replaced by a smooth sheet which conducts in one direction only. The ratio of the backward-wave impedance to the forward-wave impedance will be in the ratio  $(E_b/\beta_b)^2/(E_f/\beta_f)^2$ , where  $E_b$  and  $\beta_b$  are the longitudinal field and the phase constant for the backward wave and  $E_f$  and  $\beta_f$  are the longitudinal field and the phase constant for the forward wave. It should be noted that energy associated with spatial harmonics will reduce the forward-wave impedance to a value lower than that of Fig. 8.

It may seem odd that the impedance as a function of  $\omega/\omega_0$  does not depend on  $y_0$ , while  $\theta$  as a function of  $\omega/\omega_0$  does. This is not primarily because the capacitive loading of the ridge, which will reduce the impedance somewhat below the values calculated, has been neglected. From (3.7) we see that increasing  $\beta$ ,  $v_g$  or  $W_E$  decreases the impedance. When we increase  $y_0$ ,  $\beta$  is decreased but  $v_g$  is increased. We see from (3.6) that decreasing  $\beta$  increases  $W_E$ . It all works out that, with the approximations made, impedance is independent of  $y_0$ .

Acknowledgment:

The work presented here was done under Office of Naval Research Contract Nonr-687(00), jointly supported by the United States Signal Corps, Air Force, and Navy.

References:

1. A. Karp, paper to be published in the Proceedings of the I.R.E.
2. Electromagnetic Waves, S. A. Schelkunoff, Van Nostrand 1943, Chapter X.

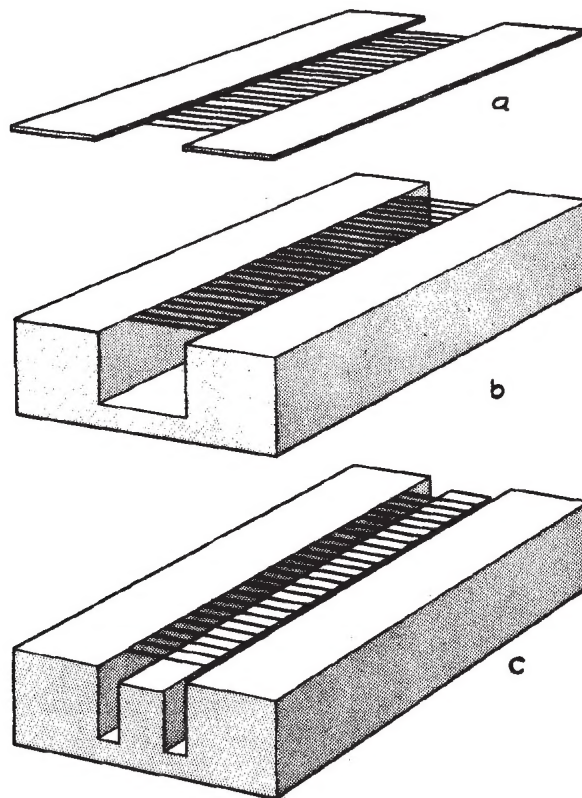


Fig. 1 - (a) An array of wires bridging the gap between two planes forms a slow-wave structure.  
(b) The wires may bridge a rectangular groove in a conducting block.  
(c) A circuit with a broader band is obtained by adding a central bar or ridge close to the wires.

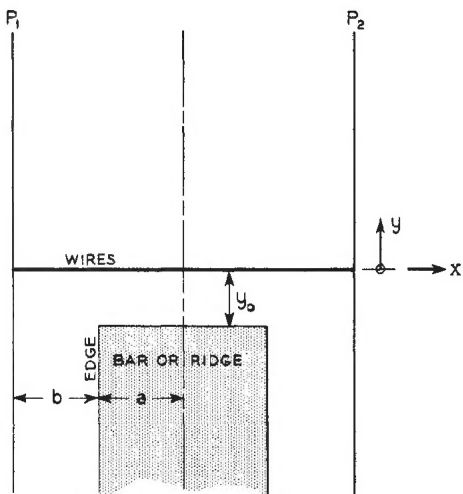


Fig. 2 - The case analyzed is that of a plane which conducts in the x direction only (representing the wires) normal to conducting planes  $P_1$  and  $P_2$  which extend in the y and z directions. A central bar with its face  $y_0$  from the wires lies below the wires.

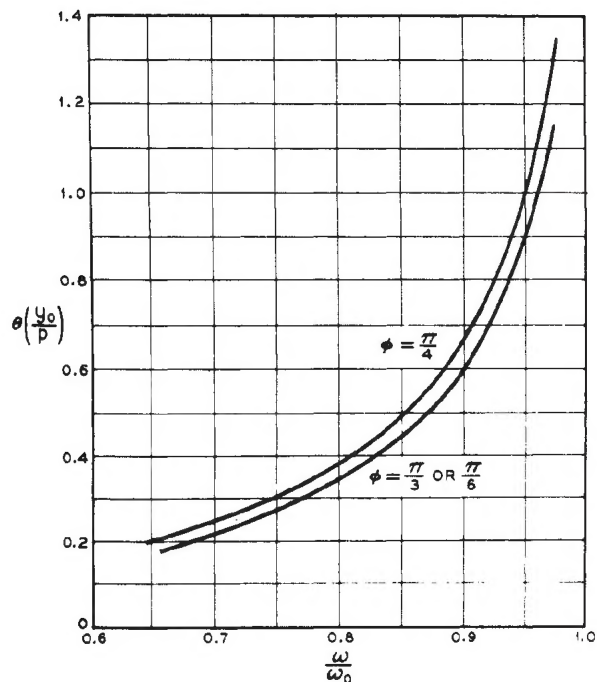


Fig. 3 - The phase vs. frequency curve for the structure of Fig. 2. Here  $\theta(y_0/p)$  where  $p$  is the pitch or distance between wires, is plotted vs  $\omega/\omega_0$ , where  $\omega_0$  is the radian frequency at which the wires are a half free-space wavelength long.

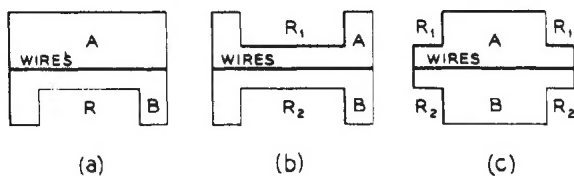


Fig. 4 - Instead of the forward-wave structure of a or b we can have backward-wave structures with central groove instead of a central bar, as shown in c.

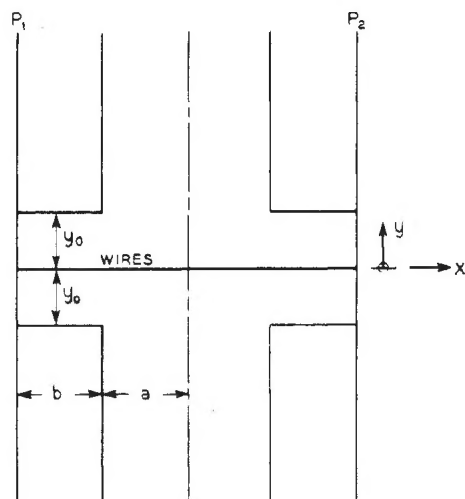


Fig. 5 - The symmetrical backward-wave structure analyzed.

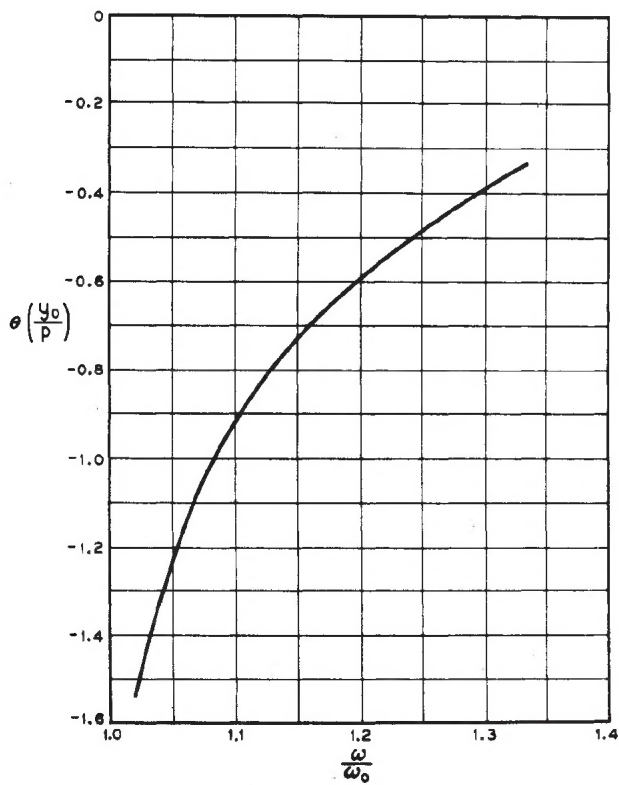


Fig. 6 - Phase curve for the structure of Fig. 5.

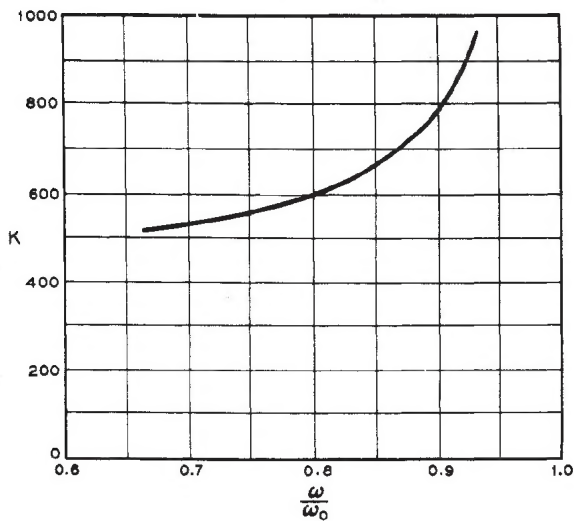


Fig. 8 - Impedance vs. frequency for the forward-wave circuit.

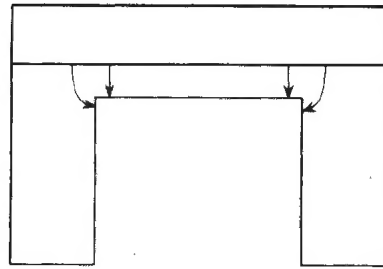


Fig. 7 - Fringing electric fields near the edges of the central bar.

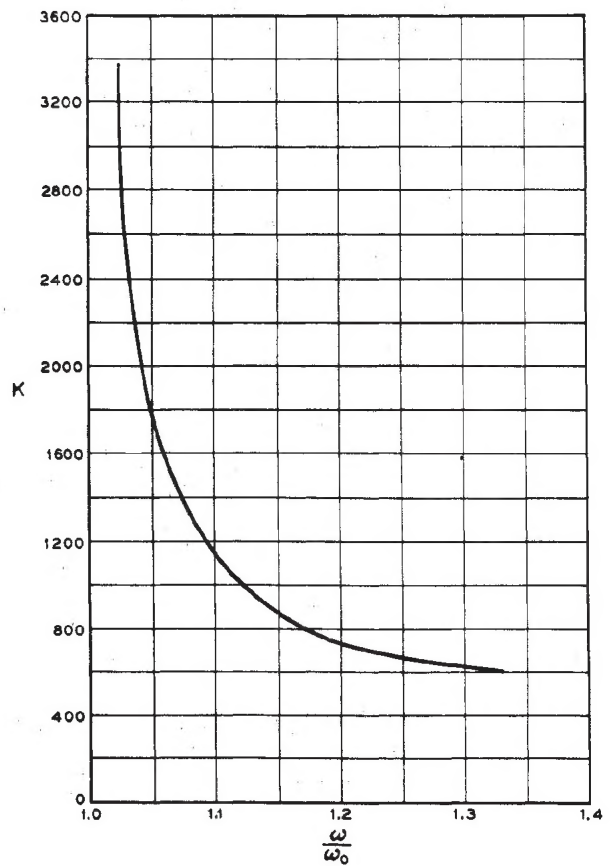


Fig. 9 - Impedance vs. frequency for the backward-wave circuit.